Calculated and measured ratios of the on-axis intensity at time t to that at $t=0$ for several of the cases investigated experimentally are shown in Fig. 3. For the parameters corresponding to the experimental conditions the approximate solution given by Eq. 6 is good for pressures down to about 50 Torr. The values of the smallness parameter $K_2 I_0$ are sufficiently large for lower pressures that the expansion to second order is no longer adequate and a numerical integration of Eq. 4 has been used. The intensity error bars on the experimental data points are the standard deviations determined by the precision of the measurements from the scan photographs. Not included is the uncertainty resulting from fluctuations in laser power at the entrance to the absorption cell. These graphs show an agreement between the experimental data and the approximate eikonal calculations for the on-axis intensity which is surprisingly good quantitatively in view of the experimental evidence regarding the validity of the paraxial approximation throughout the propagation path.

In summary, we have experimentally observed the time-dependent distortion of the intensity distribution of a 10.6-μ beam resulting from thermal blooming and convective mass flow as it propagates through CO_2 gas. An approximate solution for the expected intensity distribution based on an eikonal treatment made in the paraxial limit has been obtained for the early times when thermal blooming is dominant. In spite of the experimental evidence that the paraxial approximation is not valid over the entire propagation path for the times of interest, good qualitative agreement between the experimental and calculated intensity distributions has been observed. Furthermore, comparison of the time dependence of the experimental and calculated on-axis intensities shows good quantitative agreement. Further investigation of the intensity distribution resulting from thermal blooming is continuing.

The authors wish to express their appreciation to K.H. Wrolstad, M. Applegate, and B. Trebilcock for their assistance in this investigation.

---

†This work was supported in part by the Advanced Research Projects Agency.

[1]F.C. Gebhardt and D.C. Smith, Appl. Phys. Letters 14, 52 (1969).

[2]E.C. Cassidy and D.H. Tsai, J. Res. Nat. Bur. Stand.—C. Engineer. Instrum. 67C, No. 1 (1963).

[3]J.R. Kenemuth and M. Applegate (unpublished).

[4]K. Gullberg, B. Hartmann, and B. Kleman, Arkiv Fysik 37, 362 (1968).

[5]E.T. Gerry and D.A. Leonard, Appl. Phys. Letters 8, 227 (1966).

[6]M. Born and E. Wolf, *Principles of Optics* (Pergamon Press, Ltd., Oxford, 1965) 3rd rev. edit.

[7]D.C. Smith, IEEE J. Quantum Electron. QE-5, 600 (1969).

$CaMoO_4$ ELECTRONICALLY TUNABLE OPTICAL FILTER*

S.E. Harris and S.T.K. Nieh

Microwave Laboratory, Stanford University, Stanford, California 94305

and

R.S. Feigelson

Center for Materials Research, Stanford University, Stanford, California 94305

(Received 29 June 1970)

The paper describes a $CaMoO_4$ transmission-type acousto-optic filter. Tuning from about 6700 to 5100 Å is obtained by changing an acoustic frequency from 40 to 68 MHz. The filter bandwidth is 8 Å at an $f/6$ aperture. 95% transmission is obtained at an acoustic power density of 69 mW/mm^2.

This letter reports experimental results on a traveling wave nonresonant version of the electronically tunable acousto-optic filter.[1,2] The filter makes use of $CaMoO_4$,[3,4] which, as a result of its relatively small birefringence[5] ($\Delta n \simeq 0.01$) and low acoustic shear velocity[6] ($V = 2.95 \times 10^5$ cm/sec) allows the visible spectrum to be tuned by changing the frequency of an incident acoustic wave from about 40 to 100 MHz. The half-power bandwidth of the filter for a crystal length of 3.5 cm is about 8 Å (at 6328 Å), and 95% peak (corrected) transmission has been obtained at an acoustic power density of about 60 mW/mm^2 and an aperture of about $f/6$.

The construction of the filter is shown schematically in Fig. 1, and allows an incident optical wave

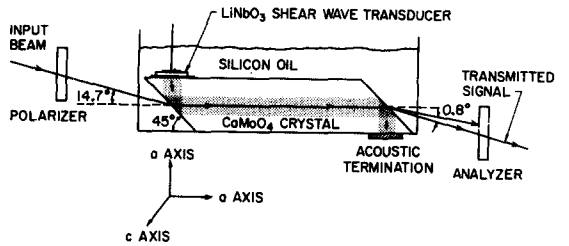

FIG. 1. Schematic of $CaMoO_4$ acousto-optic filter.

and an acoustic shear wave to propagate collinearly down the a axis of the $CaMoO_4$ crystal. The acoustic shear wave is polarized along the c axis of the crystal and acts through the p_{45} photo-elastic coefficient to couple or diffract light from one polarization into the orthogonal polarization.[7] At a given acoustic frequency, only light in a small band of frequencies satisfies $\bar{k}$ vector matching and is cumulatively diffracted and transmitted through the output analyzer. As shown in Fig. 1, the incident acoustic shear wave is brought in through a $LiNbO_3$ shear wave transducer[8] and is reflected at a 45° interface to travel collinearly with the light. Since a $CaMoO_4$ air interface has a critical angle of 30°, in order to bring the acoustic wave in at a right angle, it is necessary to use an optical index matching oil. This oil (Cargille No. 42, $n = 1.63$) has a sufficiently low acoustic impedance that the acoustic shear wave is in essence completely reflected at the interface. The acoustic wave is terminated with an epoxy and brass load. At the output interface of the $CaMoO_4$ crystal there is a small double refraction angle (about 0.8°) between the orthogonally polarized acoustically diffracted and the undiffracted portions of the incident beam. The

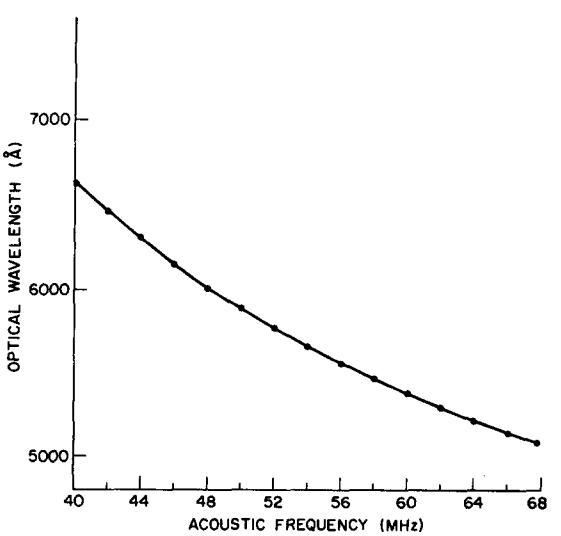

FIG. 2. Optical wavelength versus acoustic frequency.

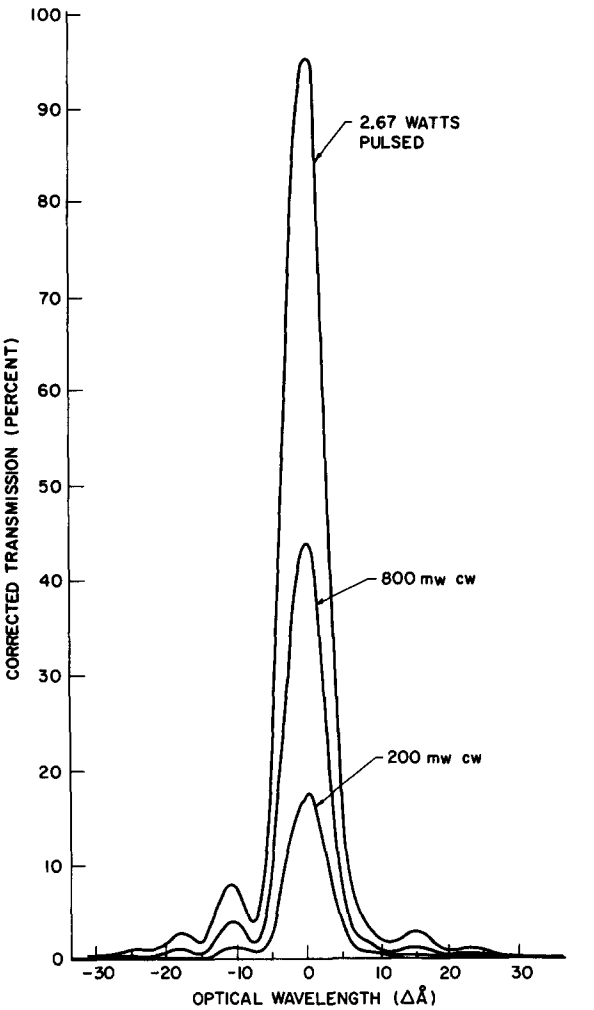

FIG. 3. Corrected transmission versus optical wavelength. True transmission is obtained by multiplying the corrected transmission by 0.78.

$CaMoO_4$ crystal was 3.5 cm long and the $LiNbO_3$ transducer had a diameter of 3 mm. The $LiNbO_3$ transducer had a half-power band pass of 20 MHz and a center frequency conversion loss of 7.5 dB.

The experimental tuning curve of the filter, as a function of the acoustic frequency, is shown in Fig. 2. Further tuning was limited by the bandwidth of the acoustic transducer, and is in principle possible over the transparency range of the material (0.4–4.5 μ).

The transmission of the filter versus optical frequency is shown in Fig. 3 for operation at different electrical powers. For these measurements the filter was tuned to 6328 Å, at which frequency the acoustic transducer was designed to center, and peak transmission was measured with a He-Ne laser. The shape of the pass band was then measured with a mercury arc source and a Spex monochromator. Since the components of the filter were not antireflection coated, the transmission scale of Fig. 3 was corrected to account for opti-

cal losses. True transmission is obtained by multiplying the corrected transmission by 0.78. For cw operation the highest corrected peak transmission which could be obtained was about 48% (37.5% measured transmission). Above this level, heating from the acoustic transducer would broaden the band pass and reduce the efficiency. Under pulsed conditions about 95% corrected peak transmission could be obtained. The average filter rejection against optical wavelengths far removed from band center was about 43 dB. The shape of the filter band pass was found to be insensitive to optical angular aperture until the external geometrical aperture of about $f/6$ was reached. Theoretically, an optical aperture of $f/5$ should result in about a 25% broadening of the half-power band pass.[9]

Based on our acoustic transducer loss, the measured transmission, necessary electrical power, crystal length, and transducer area, we estimate the photo-elastic constant $p_{45} \simeq 0.06$. This value is somewhat uncertain since at these low acoustic frequencies the near field of the acoustic transducer extended over the full length of the $CaMoO_4$ crystal and resulted in both transverse and longitudinal variations in the acoustic intensit [10] This value of p_{45} implies that 100% transmission for a 5-cm-long crystal at 5000 Å should be obtainable at an acoustic power density of 20 mW/mm^2.

The authors gratefully acknowledge Bob Griffin and Forrest Futtere for the fabrication and bonding of the acoustic transducers; and thank John Larson and Jim Young for many helpful suggestions and comments.

---

*The work reported in this letter was sponsored by the Office of Naval Research.

[1]S.E. Harris and R.W. Wallace, J. Opt. Soc. Am. 59, 744 (1969).

[2]S.E. Harris, S.T.K. Nieh, and D.K. Winslow, Appl. Phys. Letters 15, 325 (1969).

[3]T.A. Davis and K. Vedam, J. Opt. Soc. Am. 58, 1446 (1968).

[4]D.A. Pinnow, L.G. Van Uitert, A.W. Warner, and W.A. Bonner, Appl. Phys. Letters 15, 83 (1969).

[5]W.L. Bond, J. Appl. Phys. 36, 1674 (1965).

[6]W.J. Alton and A.J. Barlow, J. Appl. Phys. 38, 3817 (1967).

[7]R.W. Dixon, IEEE J. Quantum Electron. QE-3, 85 (1967).

[8]A.W. Warner, M. Onoe, and G.A. Coquin, J. Acoust. Soc. Am. 42, 1223 (1966).

[9]S.E. Harris and S.T.K. Nieh (unpublished).

[10]H. Seki, A. Granato, and R. Truell, J. Acoust. Soc. Am. 28, 230 (1956).

PIEZOELECTRIC LEAKY SURFACE WAVE IN $LiNbO_3$

A. Takayanagi, K. Yamanouchi, and K. Shibayama

Research Institute of Electrical Communication, Tohoku University, Sendai, Japan

(Received 9 March 1970; in final form 28 July 1970)

Velocities and attenuations of piezoelectric leaky surface waves in $LiNbO_3$ are computed. As the result, we have found that the effective electromechanical coupling coefficient of the leaky surface wave propagating along the x axis of the 64° rotated y-cut plane is very large, $K^2 = 0.113$; and by radiating the energy into the solid this wave attenuation is 0.36 dB/wavelength for the free surface and goes to zero for the metalized surface.

Recently $LiNbO_3$ crystals have received much attention because they have a low-acoustic surface wave attenuation and a large electromechanical coupling coefficient. Therefore, delay lines with small insertion losses and surface wave amplifiers with a large gain in combination with suitable semiconductor materials are expected, as seen in several references.[1,2] Campbell and Jones[3] discussed optimum crystal cuts and propagation directions for an effective coupling of $LiNbO_3$, which is based on the computation of the difference between a velocity of the surface wave in a free surface and that in a metalized surface. On the other hand, the investigation of the leaky surface wave consists of coupled modes involving terms decaying beneath the free surface and a term representing a bulk wave radiating into the solid.

Here, we report the computation results for the leaky surface wave coupled piezoelectrically in $LiNbO_3$. The values of the elastic and piezoelectric constants of $LiNbO_3$ were taken from the work of Warner, Onoe, and Coquin.[5] The calculated velocities are significant to 0.01 m/sec, and the attenuation to 10^{-5} dB/wavelength. We consider the waves propagating along the X axis of the rotated Y-cut plane. Figure 1 shows curves of velocities versus rotating angle for two transverse waves, Rayleigh wave and a leaky surface wave. In this figure the solid line indicates the velocities of the surface wave in the free surface adjoining vacuum